Catalysts **2013**, *3*, 176-188; doi:10.3390/catal3010176

OPEN ACCESS

Catalysts

ISSN 2073-4344

www.mdpi.com/journal/catalysts

Article

A Comparative Study on the Homo-, Co- and Ter-Polymerization Using Ethylene, 1-Decene and *p*-Methylstyrene

Dong Jin Yang, Hyun Jun Kim and Dong Hyun Kim *

Convergent Technology R&D Division, Korea Institute of Industrial Technology, Ansan-si, Korea; E-Mails: ydj0115@kitech.re.kr (D.J.Y.); mpt21@kitech.re.kr (H.J.K.)

* Author to whom correspondence should be addressed; E-Mail: dhkim@kitech.re.kr; Tel.: +82-31-8040-6226; Fax: +82-31-8040-6239.

Received: 21 December 2012; in revised form: 1 February 2013 / Accepted: 7 February 2013 / Published: 22 February 2013

Abstract: We synthesized polyethylene (PE), poly(ethylene-*co*-1-decene), poly(ethylene-*co*-*p*-methylstyrene) and poly(ethylene-*ter*-1-decene-*ter*-*p*-methystyrene) using a *rac*-Et(Ind)$_2$ZrCl$_2$ metallocene catalyst and a methylaluminoxane cocatalyst system. The materials were characterized using nuclear magnetic resonance spectroscopy and Fourier transform infrared spectroscopy. We compared and studied the kinetics, thermal properties and mechanical ones of these polymers. T_g was related to the amorphous phase of the polymers, whereas the tensile strength and storage modulus (E') were related to the crystalline phase. We also found that PE has the highest crystallinity through differential scanning calorimetry and wide-angle X-ray scattering analysis. The polymerization rates of poly(ethylene-*co*-1-decene) and poly(ethylene-*ter*-1-decene-*ter*-*p*-methystyrene) were always higher than that of polyethylene.

Keywords: metallocene catalysts; homopolymer; copolymer; terpolymer

1. Introduction

Research on polymerization using metallocene catalysts began with the identification of the structure of ferrocene by Wilkins and Fischer in 1952 and was further developed by Kaminsky in the 1980s. In the case of copolymerization using metallocene catalyst, preparing polymers with narrow molecular weight distribution, high stereo-regularity and uniform comonomer incorporation is much

easier than is the case when using a conventional Ziegler-Natta catalyst. That is the reason why many studies have been performed regarding coordination polymerization using metallocene catalysts [1].

Polyolefins are difficult to adhere and compatible with other polar polymers, because they are non-polar. The needs for improving compatibility and adhesion of polyolefins have been very high in the industry.

Theoretically, there are three possible approaches to the functionalization of polyolefins. They include (a) direct polymerization of α-olefins with functional monomers; (b) chemical modification of the preformed polymer and (c) a reactive copolymer approach that entails incorporating reactive comonomers that can be selectively and effectively interconverted into functional groups.

The third approach is a relatively new one. However, studies on the polyolefins with reactive groups have been limited, even though it may be possible to use the terpolymers to develop new high-functional polyolefins [2–5]. T. C. Chung *et al.* reported on the terpolymerization of ethylene, 1-octene and *p*-methylstyrene (*p*-MS) using $[C_5Me_4(SiMe_2NtBu)]TiCl_2$ metallocene catalyst [6,7].

In this study, we prepared polyethylene (PE), poly(ethylene-co-1-decene) (PED), poly(ethylene-*co*-*p*-methylstyrene) (PEM) and poly(ethylene-*ter*-1-decene-*ter*-*p*- methylstyrene) (PEDM) using a bridged metallocene catalyst and a cocatalyst system. We then characterized and compared with various properties of the polymers.

2. Results and Discussion

2.1. Homo-, Co- and Ter-Polymerization

Figure 1 shows a scheme for the synthesis of PEDM, PED, PEM, PE using *rac*-$Et(Ind)_2ZrCl_2$ and methylaluminoxane (MAO) as a catalyst and cocatalyst, respectively. Generally, the most interesting aspect of these zirconocene–MAO catalytic systems is the production of random copolymers with higher catalytic activities. The C2 symmetric metallocene catalyst, *rac*-$Et(Ind)_2ZrCl_2$, has a relatively electron-rich indenyl ligand. This electron-rich ligand stabilize transition metals in catalyst with cationic character, which leads to a higher catalytic activity for *rac*-$Et(Ind)_2ZrCl_2$, compared to that of other complexes.

Table 1 reports the results of homo-, co- and ter-polymerization using a metallocene catalyst/cocatalyst system under the same conditions of catalyst content, Al/Zr molar ratio, polymerization time and polymerization temperature. The catalytic activities of PED and PEDM were higher than that of PE. The catalytic activity of PED went up 2.7 fold values more than that of PE. This was attributed to the "positive" comonomer (1-decene) effect: (1) enhanced solubility of the copolymer (PED) in comparison with that of the homopolymer (PE), which favored monomer diffusion to the active center; (2) comonomer activation of new catalyst sites by increased affinity for the metallocene catalyst; and (3) increased solubility of the monomer in the liquid phase, due to the presence of the comonomer, which increased its insertion rate [8].

In the case of the terpolymer, the catalytic activity is lower than that of the copolymer (PED). This may have been due to the "negative comonomer (*p*-MS) effect." We can infer that, after the incorporation of *p*-MS into the terpolymer, its bulkiness made further insertion of ethylene and

1-decene difficult. This could also be confirmed by the very low catalytic activity of PEM, which was a copolymer of ethylene and *p*-MS, as shown in Table 1.

Figure 1. Scheme for the synthesis of homo-, co- and ter-polymer.

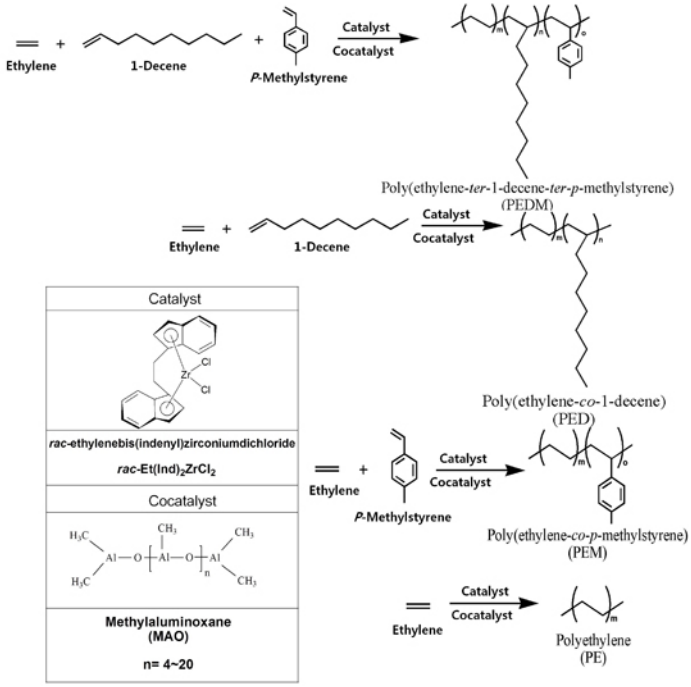

Comparing with the experimental results of T. C. Chung *et al*. [6], where they synthesized poly(ethylene-*ter*-1-octene-*ter*-p-MS), the composition of 1-octene in the terpolymer was higher than that of PEDM. It can be explained by the higher chain length of 1-decene than that of 1-octene. Also, composition of p-MS in the terpolymer was more than five-times that of PEDM. This means the bulky aromatic monomer is difficult to insert into *rac*-Et(Ind)$_2$ZrCl$_2$, which has a narrower bond angle than [C$_5$Me$_4$(SiMe$_2$NtBu)]TiCl$_2$.

Figure 2. Fourier transform infrared (FT-IR) spectra of (**a**) insoluble parts after Soxhlet processing with hexane for poly(ethylene-*ter*-1-decene-*ter-p*- methylstyrene) (PEDM) and (**b**) polyethylene (PE).

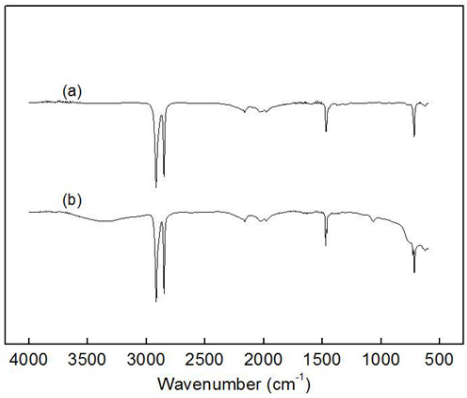

Table 1. Results for homo-, co- and ter-polymerization.

NAME [a]	Feeding			E:D:M Feed Molar ratio	Composition			Catalytic Activity (kg of polymer/(mol·h))	M_w [d] (kg/mol)	M_n [d] (kg/mol)	MWD [d]
	E [b] (mol/L)	D [b] (mol/L)	M [b] (mol/L)		E [b,c] (mol %)	D [b,c] (mol %)	M [b,c] (mol %)				
PE	0.4	0	0	1:0:0	100	0	0	1420	-	-	-
PED	0.4	0.4	0	1:1:0	79.8	20.2	0	3840	100	29	3.4
PEM	0.4	0	0.4	1: 0:1	98.9	0	1.1	350	85	26	3.3
PEDM	0.4	0.4	0.4	1: 1:1	65.4	33.4	1.2	2648	100	37	2.7

[a] Polymerization conditions: catalyst = 2.5 μmol (*rac*-Et(Ind)$_2$ZrCl$_2$), Al/Zr = 3,000, polymerization time = 30 min, polymerization temperature = 50 °C and solvent = toluene; [b] E = Ethylene, D = 1-decene, M = *p*-MS; [c] Determined by ^{1}H-NMR spectroscopy; [d] Determined by gel permeation chromatography (GPC).

2.2. Characterization

Figure 2 shows two kinds of Fourier transform infrared (FT-IR) spectra: (a) the spectrum of insoluble parts produced through the Soxhlet process using n-hexane for PEDM and (b) the spectrum of PE. The spectra of (a) and (b) have very similar peaks. This result indicated that both of the polymers were homo-polyethylene and the polyethylene, which occurred during the terpolymerization and was efficiently eliminated through the Soxhlet process. The C-H stretching peaks mutually appear near 2850 cm^{-1} and 2950 cm^{-1}. The CH_2 bending peak and out of plane C-H bending are near 1400 cm^{-1} and 720 cm^{-1}, respectively. We concluded with certainty that, through the Soxhlet process, we separated the by-product (homo-polyethylene) from the terpolymer.

Figure 3. ^{1}H NMR spectrum for the terpolymer (PEDM).

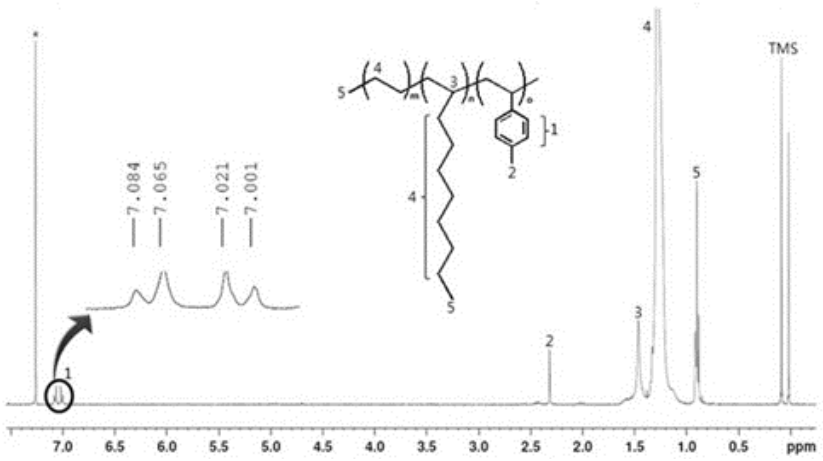

Figure 3 is the ^{1}H NMR spectra of PEDM. The signatures near 7.0 ppm correspond to the aromatic peaks of *p*-MS. The peaks for the CH, CH_2 and CH_3 of ethylene or 1-decene appear in the range 0–3 ppm. The peaks for the CH_3 of the 1-decene/ethylene and *p*-MS were near 0.9 ppm and at 2.3 ppm, respectively. The peak for the CH of the 1-decene was near 1.5 ppm. Compared with the peaks for the CH_3 of *p*-MS, the CH_3 of 1-decene or ethylene occupied a relatively broad area. We can confirm the insertion of the 1-decene and p-MS into the terpolymer by the characteristic peaks for the CH_3 of the *p*-MS and the CH of the 1-decene.

Figure 4 shows the ^{13}C NMR spectra of the PE, PED and PEDM. In the case of PEDM in particular, or*tho* and *meta* carbon atoms are present in the benzene ring. The carbon atom at the *ortho* position is *ortho* plus *meta* to the substituents, and the carbon atom at the *para* position is *meta* plus *para*, being 129.6 ppm and 133.2 ppm, respectively. The peak for the CH_3 of *p*-MS was detected at 21 ppm.

It is logical to expect that the methyl group substitution at the *para*-position will have very little effect on the chemical shifts of methylene and methine carbons in the polymer backbone. In addition to the two chemical shifts (21.01 and 29.8 ppm), corresponding to the methyl group from *p*-MS and methylene group from ethylene, respectively, there are three peaks (27.74, 37.01 and 45.77 ppm) corresponding to methylene and methane group from *p*-MS units, which are separated by multiple ethylene units along the polymer chain [9].

Figure 4. ^{13}C-NMR spectra of (**a**) PE; (**b**) poly(ethylene-co-1-decene) (PED) and (**c**) PEDM.

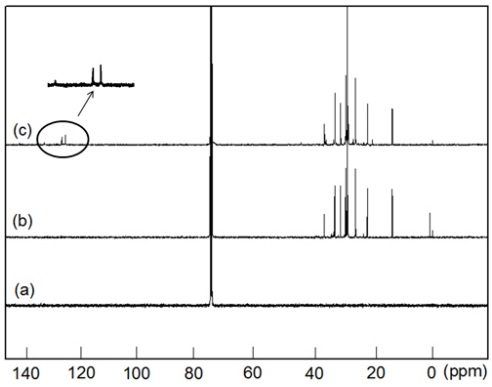

2.3. DMA

Figure 5 shows the variation in the loss tangent (tan δ) and dynamic storage moduli (E') of PE, PED and PEDM, according to the temperature.

Figure 5. Tan δ and storage moduli *versus* temperature fort (**a**) PE; (**b**) PED and (**c**) PEDM.

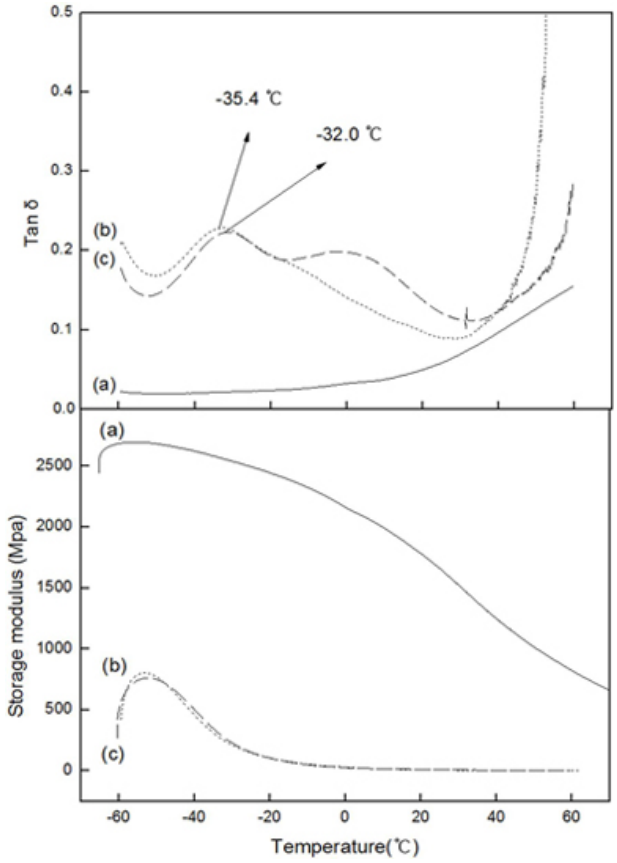

DMA is a very sensitive method for measuring the T_g value of polymers. Side-chain or main-chain motion in specific regions of a polymer and local mode relaxations, which cannot be monitored by DSC, can be observed using DMA [10]. T_g is the dominant transition in amorphous polymers or semi-crystalline polymers that are composed of amorphous regions. Because T_g occurs at the highest temperature among other transitions, it is also called the α-transition. Figure 5 show that the T_g value of PEDM and PED were –32.0 °C and –35.4 °C, respectively. The T_g value of PEDM was higher than that of PED, which could be ascribed to the rigid molecular *p*-MS feature in the terpolymer.

The dynamic storage modulus (E') is approximately similar to the Young's modulus, elastic modulus or stiffness [11]. The Young's or elastic modulus is related to the crystallinity of the polymer. The storage moduli of PEDM and PED were much lower than that of PE, which may have been due to the very low crystallinity of PED and PEDM compared with PE.

2.4. DSC

Figure 6 shows the DSC thermograms for PE, PED and PEDM. The variation in the second cooling and third heating curves of the polymers is shown in the upper and lower areas, respectively.

Figure 6. DSC (**a**) cooling and (**b**) melting thermograms of PE, PED and PEDM.

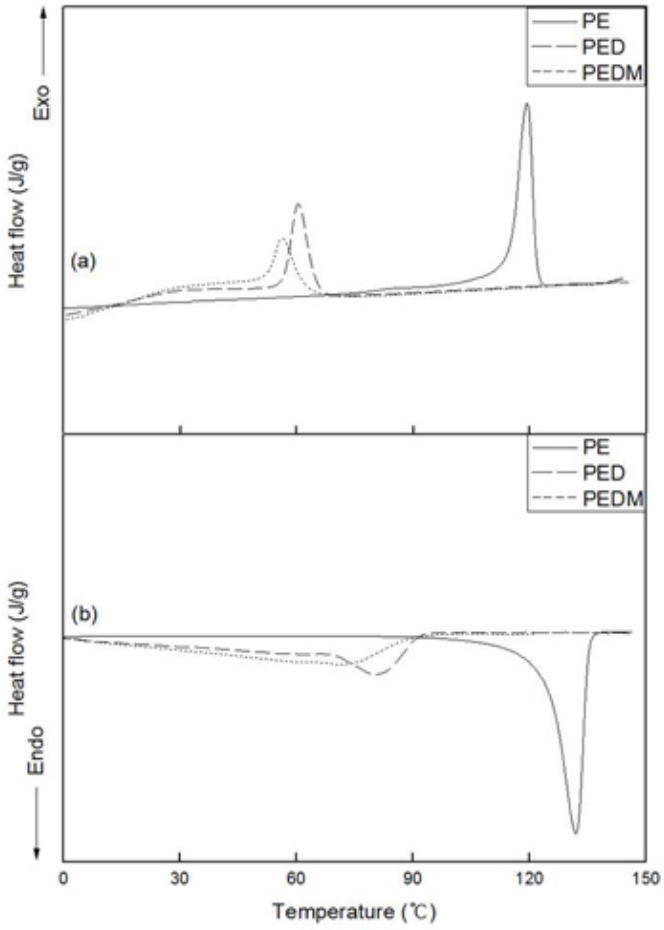

We confirmed the crystallization temperatures (T_c) and melting temperatures (T_m) of the polymers. The T_m value of PE was around 135 °C, which is similar to that of commercial high-density polyethylene.

As expected, both the T_m and T_c values of PED and PEDM showed important decreases, compared with those of PE. PEDM has higher value of T_m than PED, which was possibly due to the high crystallinity of PEDM and the contribution of the *p*-MS in the PEDM. We can explain this contribution of the *p*-MS using the experimental results of T. C. Chung *et al.*, who explored the thermal properties of the ethylene-*p*-MS copolymer. They reported a melting point of 115 °C for *p*-MS content of 1.1 mol % in the copolymer, which was very similar to *p*-MS content for our PEDM sample. This means that through the incorporation of *p*-MS in the terpolymer, we were able to raise the T_m value of the ethylene-1-decene copolymer. T_c of the polymers showed trends very similar to their T_m.

Table 2 summarizes the T_m, T_c, ΔH_m and crystallinity values measured by DSC. The crystallinities were calculated from their enthalpies of fusion. Since we were able to confirm the enthalpy of melting (ΔH_m) of PED than that of PEDM, the crystallinity of PEDM was higher than that of PED.

Table 2. T_m, T_c, ΔH_m and crystallinities of PE, PED and PEDM.

NAME [a]	T_c [b] (°C)	T_m [b] (°C)	ΔH_m [b] (J/g)	Crystallinity [b] (%)
PE	118.7	135.0	171.0	58.2
PED	58.4	79.4	3.7	1.3
PEDM	58.4	82.7	4.5	1.5

[a] Polymerization conditions: catalyst = 2.5 μmol (*rac*-Et(Ind)$_2$ZrCl$_2$), Al/Zr = 3000, polymerization time = 30 min, polymerization temperature = 50 °C and solvent = toluene; [b] Determined by differential scanning calorimetry (DSC).

2.5. WAXS

The wide-angle X-ray scattering (WAXS) data for PE, PED and PEDM are shown in Figure 7. There are three peaks in the copolymer (PED) and terpolymer (PEDM). The broad amorphous peaks near 19.5–20° appeared were due to the contribution of 1-decene. However, the broad amorphous peaks decreased as *p*-MS was inserted into the terpolymer. Two other small peaks for the copolymer and the terpolymer that were present in the 21.8° and 24.3° were identical for the crystalline homopolymer (PE). This fact indicates that the copolymer and terpolymer were partially crystalline, although the crystallinity decreased substantially with the insertion of the comonomer and termonomer.

2.6. Kinetics

Figure 8 show the polymerization rate curves for the homo-, co- and ter-polymer. All of the polymerizations were marked by very high initial rates for which the maximum rate ($R_{p,\ max}$) was reached within 1–2 min. Within this period, a pronounced change in the viscosity of the solvent was observed. Except for the polymerization curve of PEM, the reaction rates of the copolymerization and the terpolymerization were higher than that for homopolymerization at all times. This fact was ascribed to the "positive comonomer (1-decene) effect."

In the case of PEM, although the reaction rate was higher than that of PE in the beginning, the reaction rate became lower than that of PE. The reaction rate of PEDM was higher than that of PED until 12 min. after which, the reaction rate of PEDM became lower than that of PED. These observations were ascribed to the "negative comonomer (*p*-MS) effect." This negative comonomer

effect could be explained by the fact that *p*-MS that was inserted into the copolymer or terpolymer disturbed additional incorporation of other monomers [12,13].

Figure 7. Wide-angle X-ray scattering data for (**a**) PE; (**b**) PED and (**c**) PEDM at room temperature.

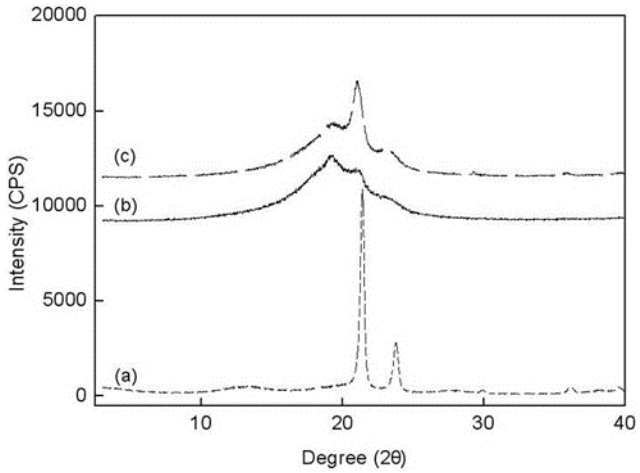

Figure 8. A comparison of the polymerization rate (R_p) curves according to the polymerization time: (**a**) PE; (**b**) PEM; (**c**) PED and (**d**) PEDM.

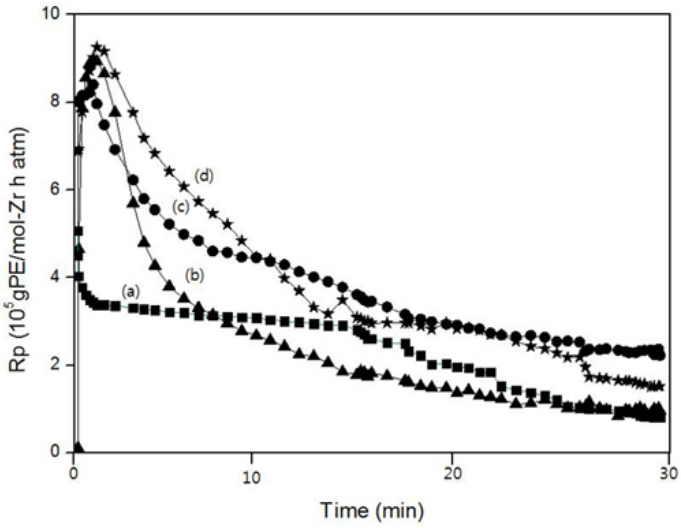

2.7. Mechanical Properties

The stress-strain behaviors of PE, PED and PEDM are shown in Figure 9. The polymers showed very different stress-strain curves. PE had a very high elastic modulus and exhibited typical ductile plastic fracturing with a marked yield point, which was related to its low degree of branching and high crystallinity. On the other hand, PED and PEDM underwent dramatically extensive plastic deformation (exceeding 1000% stain) before breaking and show elastomeric behavior with a lower modulus than that for PE. They became so rubbery that there was no longer a yield point. PEDM had higher tensile strength than PED, which was ascribed to the higher crystallinity of PEDM.

Figure 9. Stress and strain curves of (**a**) PE, (**b**) PED and (**c**) PEDM.

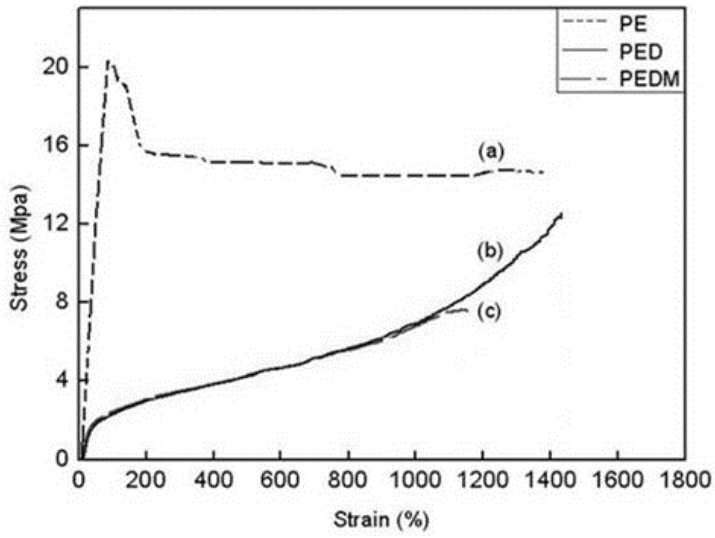

3. Experimental Section

3.1. Materials and Specimens

All manipulations were carried out in an inert nitrogen atmosphere. We used high-purity grade ethylene gas (Dae-myung Gas Co., cheonan, Korea) after passing it through an alumina/zeolite column. 1-decene (Aldrich, 94%), *n*-hexane (SAMCHUN, 99.5%,) and toluene (SAMCHUN, 99.5%) were purified by refluxing them over sodium, using benzophenone as an indicator and stored in a dry box. A solution of *rac*-Et(Ind)$_2$ZrCl$_2$ (Sigma Aldrich, MO, USA) in toluene was also prepared. MAO (Tosho, methylaluminoxane) was used as received. *p*-methylstyrene was distilled under reduced pressure in the presence of CaH_2 after performing standard purification procedure. Specimens for the thermal, mechanical and wide-angle X-ray scattering (WAXS) analysis were prepared by compression molding in a hot press.

3.2. Polymerizations

Typically, all of the polymerization reactions were carried out in a 300 mL stainless steel autoclave with a mechanical stirrer. After the autoclave was saturated with ethylene gas, the polymerization reaction was started by the injection of the required amount of catalyst solution and MAO. After several minutes, the polymer solution was poured into a diluted HCl/EtOH solution. The resultant polymer was washed with EtOH (600 mL) and dried *in vacuo*.

Using a Soxhlet apparatus and n-hexane as a solvent, we separated each soluble copolymer or terpolymer from the insoluble polyethylene (some types of by-products). After drying the soluble fractions, we could finally obtain pure copolymer and terpolymer, which were completely soluble in common organic solvents, such as the hexane, toluene and tetrahydrofuran. Polymer yield and catalytic activity were determined by gravimetry.

3.3. Characterization

Fourier transformed infrared (FT-IR) analysis was performed by NICOLET 6700 (Thermo Scientific Co., Waltham, MA, USA).

^{13}C NMR spectra were obtained at 60 °C. The equipment that was used was AVANCE 500 MHz (Bruker, Karlsruhe, Germany). Sample solutions of the polymer were prepared in $CDCl_3$. The deuterated solvent was used to provide an internal lock signal.

^{1}H NMR spectra were recorded on AVANCE 500 MHz (Bruker, Karlsruhe, Germany). The NMR samples were prepared in $CDCl_3$ solvent at 60 °C.

The molecular weight and the molecular weight distribution of the polymers were measured using PL-GPC210 (Polymer Laboratories Co., Church Stretton, UK) gel permeation chromatography fitted with Styragel (olesis guard column) HT-type columns. This test method uses commercially available polystyrene standards. The analyses were performed at 140 °C and 1.0 mL/min with 1,2,4-trichlorobenzene as a solvent.

3.4. Dynamic Mechanical Analysis

The dynamic mechanical spectra of the samples were obtained by using a dynamic mechanical analysis (DMA) machine [Seiko Co., Exstar 6000] over the temperature range –60 to 60 °C. The specimens were analyzed in tension mode at a constant frequency of 1 Hz using 0.01% strain at a heating rate of 2 °C/min.

3.5. Differential Scanning Calorimetry

Differential scanning calorimetry (DSC) data for the terpolymer were recorded by means of a DSC7 (PERKIN ELMER Co.). Samples were heated from 0 °C to 150 °C and then cooled down at 10 °C/min to 0 °C. Following this, they were reheated at 10 °C/min to 150 °C. The crystallization temperature (T_c), melting temperature (T_m) and enthalpy of fusion (ΔH_m) were derived from the second and third run curves, respectively. The measured ΔH_m value was converted into the degree of crystallinity $(1 - \lambda)_{\Delta H}$ using 290 J/g as the enthalpy of fusion of a perfect polyethylene crystal [14].

3.6. Wide-Angle X-ray Scattering

Wide-angle X-ray Scattering (WAXS) patterns were recorded in reflection mode at room temperature using D/MAX-2200V X-ray Diffractometer (Rigaku, Tokyo, Japan) connected to a computer. The instrument used the Cu source, and it performed measurements at 40 kV and 40 mA. The diffraction scans were collected over a period of 20 min between 2 θ values from 3.0 to 40.0° at a scan rate of 2°/min.

3.7. Mechanical Property

Elastic modulus, tensile strength and elongation at break were determined with a universal testing machine (Tinius Olsen Co. Ltd., Salford, UK, H5K-T), according to ASTM method D412 at a

crosshead speed of 10 mm/min. For each film sample, measurements were made on five specimens taken from the same film, and the average of their results was reported.

4. Conclusions

Homo-, co- and ter-polymer were prepared and compared with various properties. We confirmed the synthesis of PED and PEDM using ^{1}H NMR, ^{13}C NMR and FT-IR analysis. T_g of PEDM was higher than that of PED, which is possibly due to the rigid molecular feature of the *p*-MS in the terpolymer. In the case of the storage modulus, those for PED and PEDM were much lower than that of PE, which was possibly due to the very low crystallinity of PED and PEDM. Both T_m and T_c of the PED and PEDM showed significant decreases, compared with those of PE. All of the copolymer and terpolymer were partially crystalline, although the crystallinity decreased greatly with the insertion of the comonomer and termonomer. Through a kinetic study, we ascertained that 1-decene and *p*-MS exerted a positive and negative comonomer effects on terpoloymerization, respectively. PEDM had higher tensile strength than PED, which was attributed to the higher crystallinity of the terpolymer.

In this study, we synthesized the terpolymer composed of ethylene, 1-decene and *p*-MS. 1-decene and *p*-MS are responsible for reducing the gas transition temperature of the terpolymer and reactive moiety, respectively, which could be easily converted into functional groups like -OH, -NH, -COOH, anhydrides and halogens under mild conditions. We have therefore opened up the possibility of developing new high-functional elastomers in the future.

Conflict of Interest

The authors declare no conflict of interest.

References

1. Kaminsky, W.; Sinn, H. *Transition Metals and Organometallics as Catalysts for Olefin Polymerization*; Springer-Verlag, Manasquan, NJ, USA, 1988.
2. Villar, M.A.; Ferreira, M.L. Co- and terpolymerization of ethylene, propylene, and higher α-olefins with high propylene contents using metallocene catalysts. *J. Polym. Sci. Part A* **2001**, *39*, 1136–1148.
3. Fernanda, F.; Nunes, E.; Griselda, B.G. ^{13}Carbon Nuclear Magnetic Resonance of Ethylene–Propylene–1-hexene Terpolymers. *J. Polym. Sci. Part A* **2004**, *42*, 2474–2482.
4. Griselda, B.G.; Fernanda, F.; Nunes, E.; da Silva, L.F.; Maria, M.; de Camargo, F.; Raul, Q. Ethylene–propylene-α-olefin terpolymers thermal and mechanical properties. *J. Appl. Polym. Sci.* **2007**, *104*, 3827–3836.
5. Chung, T.C.; Lu, H.L. Kinetic and Microstructure Studies of Poly(ethylene-*co*-p-methylstyrene) Copolymers Prepared by Metallocene Catalysts with Constrained Ligand Geometry. *J. Polym. Sci. Part A* **1998**, *36*, 1017–1029.
6. Lu, H.L.; Hong, S.; Chung, T.C. Synthesis of New Polyolefin Elastomers, Poly(ethylene-*ter*-propylene-*ter*-p-methylstyrene) and Poly(ethylene-*ter*-1-octene-*ter*-*p*-methylstyrene), Using Metallocene Catalysts with Constrained Ligand Geometry. *Macromolecules* **1998**, *31*, 2028–2034.

7. Chung, T.C.; Lu, H.L. Synthesis of poly(ethylene-*co*-*p*-amethylstyrene) copolymers by metallocene catalysts with constrained ligand geometry. *J. Polym. Sci. Part A* **1997**, *35*, 575–579.
8. Quijada, R.; Narvaez, A.; Rojas, R.F.; Rabagliati, M.G.B.; Galland, R.S.; Mauler, R.; Benavente, E.; Perez, J.M.; Perez, A.B. Synthesis and characterization of copolymers of ethylene and 1-octadecene using the *rac*-Et(Ind)$_2$ZrCl$_2$/MAO catalyst system. *Macromol. Chem. Phys.***1999**, *200*, 1306–1310.
9. Chung, T.C.; Lu, H.L. Synthesis of poly(ethylene-*co*-*p*-methylstyrene) copolymers by metallocene catalysts with constrained ligand geometry. *J. Polym Sci. Part A* **1997**, *35*, 575–579.
10. Hatakeyama,T.; Quinn, F.X. *Thermal Analysis*, 2nd ed.; John Wiley & Sons, Inc.: New York, NY, USA,1999; p. 131.
11. Vickroy, V.V.; Abbott, R.F. Dynamic mechanical relaxations in polyethylene. *Macromolecule* **1985**, *18*, 1302–1309.
12. Kim, I. Copolymerization of ethylene and 5-vinyl-2-norbornene by stereospecific metallocenes and epoxidation of the resulting copolymer. *React. Funct. Poly.* **2001**, *49*, 197–204.
13. Chein, J.C.W.; Noozaki, T. Ethylene–hexene copolymerization by heterogeneous and homogeneous Ziegler–Natta catalysts and the "comonomer" effect. *J. Polym. Sci. Part A* **1993**, *31*, 227–237.
14. Flory, P.J.; Vrij, A.J. Melting Points of Linear-Chain Homologs. The Normal Paraffin Hydrocarbons. *J. Am. Chem. Soc.* **1963**, *85*, 3548–3553.